EOLI ICA4-CT-2002-10012
Efficient Operation of Urban Wastewater Treatment Plant

KINETIC PARAMETER ESTIMATED VALUES FOR PARTICULAR EFFLUENTS AND REACTORS

Deliverable 2.2

Deliverable Type: Report
Number: D2.2

Contractual Date of Delivery: T_0+10
Actual Date of Delivery: 20.01.2006

WP2 - Kinetic parameter estimated values for particular effluents and reactors
Involved partners: CESAME-UCL, LBE-INRA and UNAM

Section 2 By Jaime A. Moreno and Manuel J. Betancur
Institute of Engineering, Universidad Nacional Autónoma de México (UNAM)

Abstract: This report describes the kinetic parameter estimation, for the model used in solving the problem of increasing the performance of WWTPs, for the Carbon removal case (Eoli Model 1, EM1) dealing with toxic wastewaters and for the EM2 case …

Keywords: Haldane inhibitory model, Kinetic parameters, Activated sludge WWTP, Sequencing Batch Reactor (SBR),

1.

2. Introduction

In this project, three types of wastewater are considered. The first one coming from a dairy industry, contaminated with organic carbon components as well as nitrogen. The second contains toxic or recalcitrant compounds, typical for an area including the chemical industry. The third one is a domestic wastewater which occasionally contains toxic or organic overloads. They are grouped in two model classes: one with only Carbon as the substrate to be removed (denoted EM1: EOLI Model 1), and another with Nitrogen, where nitrification and denitrification are needed (denoted EM2).

The models studied in this WP are therefore linked to the specific application. Section two presents the EM1 case that deals with the WWTP at UNAM + IBTech; while Section three is dedicated to EM2, related to the WWTP for the following partners: CESAME-UCL, LBE and POLIMI (+ENEA as subcontractor).

3. Eoli Model 1 (EM1) process: wastewater at UNAM and IBTech

A detailed explanation of the parameters estimation process may be found in the reports "EM1_AB_(WP2_unam)1.5d.doc" and "EM1_CD_(WP2_unam)1.9d.doc". An extract with the relevant results follows:

3.1. *EM1 dynamical model structure*

The process studied is related to the reaction describing the degradation of the treated substrate via aerobic digestion in a sequencing batch reactor (SBR). A process model considering the fill and react phases (settling, drawing and idling phases are not addressed here) was needed in order to study the time-optimization problem. The manipulated variable was chosen to be the inlet flow rate F_{in} into the SBR. Let us denote S_C, S_O, and X respectively, the concentration of the substrate to be treated *(also denoted simply as S in some related publications)*, the concentration of the dissolved oxygen (DO) in the water *(also denoted simply as O)* and the concentration of the biomass for the simplified reaction.

A simple mass balance leads to obtain the following EM1 equations for the Standard Operation conditions of the SBR (fill and react phases only). The assumed conditions are: acclimated biomass, not strongly inhibited, no Oxygen limitation, and bounded inflow feed rate $0 \le F_{in} \le F_{\max}$.

$$\frac{dX}{dt} = \left(\mu - \frac{F_{in}}{V}\right)X \tag{1}$$

$$\frac{dS_C}{dt} = -k_1 \mu X + \frac{F_{in}}{V}\left(S_{C,in} - S_C\right) \tag{2}$$

$$\frac{dS_O}{dt} = -\left(k_2 \mu + b\right)X + \frac{F_{in}}{V}\left(S_{O,in} - S_O\right) + k_L a\left(S_{O,sat} - S_O\right) \tag{3}$$

$$\frac{dV}{dt} = F_{in} \tag{4}$$

where k_1, k_2, μ, b, $k_L a$, $S_{C,in}$, $S_{O,in}$, $S_{O,sat}$ and V are, respectively, the yield coefficient for substrate degradation *(also denoted as $1/Y_{x/s}$ or simply $1/Y$)*, the oxygen yield coefficient *(also*

denoted as $1/Y_{x/o}$), the specific biomass growth rate, the specific endogenous respiration rate of the biomass in the water *(also denoted as r)*, the oxygen mass transfer coefficient, the influent substrate concentration *(also denoted as S_{in} or simply S_i)*, the influent DO concentration *(also denoted as O_{in} or simply O_i)*, the saturation DO concentration in the liquid medium *(also denoted as O_{sat} or simply O_s)* and the volume level of the wastewater being treated in the SBR tank.

As the substrate inhibits the biomass growth, a Haldane type model can be applied to approximately describe the specific growth rate of the biomass:

$$\mu = \frac{\mu_{\max} S_C}{K_S + S_C + \frac{S_C^{\,2}}{K_I}} \quad \text{if } S_C \geq S_t \tag{3}$$

$$\mu = \mu_t \frac{S_C}{S_t} \quad \text{if } S_C < S_t \tag{6}$$

Where the kinetic parameters $\mu_{\max}$, K_S and K_I are the specific biomass growth rate coefficient *(also denoted as μ_o)*, the Michaelis-Menten affinity constant and the inhibition constant, respectively; and S_t is a threshold value that allows to modify the early part of the Haldane kinetics replacing it by a linear non-inhibitory kinetics of slope μ_t/S_t.

3.2. *EM1 kinetic parameter estimation process*

3.2.1 **Model Configuration**

Different configurations were considered for the parameter calibration e.g. with or without inlet dissolved oxygen presence, with or without sensor dynamics, with or without the modification of the early (non-inhibitory) part of the Haldane kinetics. The final configuration chosen was the denoted as EM1-A3 in the reports. It captures all of the basic behavior of the process keeping the model complexity to a minimum i.e. no sensor dynamics considered, no inlet dissolved oxygen assumed ($S_{O,in} = 0$) and no modification of the classical Haldane kinetics ($S_t = 0$) in Equation (5).

3.2.2 **Estimation methodology**

After separating the experiments in two groups (identification and validation) the calibration process was applied to each experiment in the identification group. Afterwards a statistical analysis was applied to each set of parameters in order to find their mean values and the confidence intervals.

In order to identify the kinetic parameters the MatLab “lsqnonlin” function was used. For doing this, a series of Matlab m-files were written. Both Levenberg-Marquardt and Gauss-Newton algorithms were tested. No significant difference was found in the results. The versions of the software used were: MATLAB Version 6.5.0.180913a (R13) and Optimization Toolbox Version 2.2 (R13).

3.3. *Results*

3.3.1 **Wastewater and bioreactor description**

For the organic toxic wastewater model compound a synthetic wastewater was used. It contained 4-chloro-phenol (4CP) as the sole energy source. Nutrients (nitrogen and phosphorous) and oligo-elements were added as recommended by AFNOR (1985).

The SBR used was a lab-scale reactor with a maximum volume of 7 liters and a 4 liters exchange volume.

3.3.2 **Estimated parameters**

Table I presents the estimation results for the kinetic parameters. All other parameters are also presented for completeness.

Table I – Parameter estimation results for EM1-A3 model

EM1 candidate results		b	K_La	k_1	k_2	μ_o	K_I	K_S
Units		h^{-1}	h^{-1}	*mg4CP/mgVSS*	*mgDO/mgVSS*	h^{-1}	*mg4CP/L*	*mg4CP/L*
EM1-A3	Confidence Interval 95%	0.0004	0.1		0.0578	0.00255	0.00755	0.01499
	Confidence/Mean ratio	7%	1%		6%	1%	0%	0%
	Mean Value	0.0059	16.8	3.7	1.0363	0.1916	3.75305	60.0076

3. EOLI Model 2 (EM2)

3.1 Materials and methods

3.1.1 Reactor design and start up phase

Activated sludge:
The sludge used in the LBE SBR comes from the urban wastewater treatment plant of COURSAN, south of France. This plant was chosen because both carbon and nitrogen are treated in aerobic and anoxic conditions. The tank was filled with about 100 litters of this sludge. For two month, the sludge was simply aerated and filled with a low organic loading rate (<0.7 kg COD/m^3/day). After three months of start up, the purification rate was around 98% and a high sludge settleability with no suspended solid after decant was obtained.

Influent wastewater
Semi-synthetic dairy wastewater is used as influent. This fed is prepared by dilution of concentrated whey collected in a cheese dairy. The characteristics of the whey correspond to 70 g/L of COD and 2 g/L of Total Kjedahl Nitrogen (NTK). In order to change the C/N ratio of the whey, organic nitrogen as Urea (CH_4N_2O) is added.

The whey is maintained at –20°C in small bottles. About 3.6 litres are used per day to prepare reactor's feed. In standard conditions, the influent volume treated after dilution is 50 l/day. Its average composition is : 5 g/L COD, 250 mg/L N-NTK, *and pH = 6,23.

Pilot plant
The tank of the reactor has a cylindrical form. Its dimensions are 50cm ∅ and 130cm height with a total volume of 255L. It is equipped with a variable flow rate pump to fill the reactor and a controlled valve to withdraw the effluent and the sludge in excess. Air is used for aeration and mixing. Its flow is controlled by a flow meter.

The reactor is operated at an ambient lab temperature of 20°C. Each cycle duration is 24 hours. More specifically, the reaction phases are divided into 2 periods. In each one, half of the total influent daily volume is added (25 liters).

3.1.2 Measurements

On line data
The following parameters are available on line : pH, Redox, Temperature, Dissolved Oxygen (DO), CO_2 gas, O_2 gas, sludge blanket, influent air flow rate and input air flow rate. All sensors and actuators are connected to a PC and the functioning of the process is completely automated. The on-line measurements are captured by an integrated computer system developed within the EOLI WP8.

Off line data
The off line measurements are : COD (total and soluble), NTK, Nitrite, Nitrate, Ammonium, TSS and VSS. For all these measurements, standard methods are used.

3.1.4 Experimental data sets used for model identification

9 data sets were used for identification purposes. They group data obtained under very different input and aeration conditions. General characteristics of these experimental data are reported in Table 1.

Table 1: General environmental characteristics of the data sets used for model identification

File name (date)	Total COD input (mg/L)	TKN input (mg/L)	SVM (g/L)
12112003	5,501	285	15.2
08072003	4,781	285	12.6
06112003	4,800	260	11.5
04112003	5,970	319	14.4
29102003	5,280	183	13.1
26062003	3,045	252	10.6
15042004	3,630	207	15.0
10072003	7,009	257	10.8
06082003	6,456	280	13.8

Let X_1 and X_2 be the concentrations of the biomass growing on carbon and nitrogen, respectively. A number of parameters of the models developed hereafter, as Y_1 (yield coefficient for the production of X_1 : g of X_1 per g of degraded COD), Y_2 (yield coefficient for the production of X_2 : g of X_2 created per g of degraded TKN), α (yield coefficient for the production of NO_x : g of NO_x produced per g of degraded TKN), as well as the terms S_o^{SA} (saturation value for the dissolved oxygen concentration which includes the endogenous

respiration) and k_La (oxygen transfer coefficient) are calculated for each data sets following the general rules recalled hereafter.

First, using all available data, it was established that the mean total biomass production by volume unit and by the quantity of degraded COD was 0.0019 gMES/L/gCOD. Then, it was verified that the ratio VSS/SS was constant for all considered experiments. It was found that this ratio equals 0.8±0.04. Furthermore, according to the literature, it was assumed that the carbon oxidizers micro-organisms represented 90% of the MVS and the nitrogen oxidizers micro-organisms, 10%. Assuming that the total biomass concentration (MVS) we have for each data set is the final value (afterwards, the biomass does not change anymore), we can compute the initial theoretical values for X_1 and X_2. From these additional data, using the environmental characteristics reported for each data set in the table 1, we are able to compute the other parameters as :

$$Y_1 = \frac{\Delta X_1}{\Delta COD} \ (\text{g}X_1\text{/L/gCOD/L})$$

$$Y_2 = \frac{\Delta X_2}{\Delta TKN} \ (\text{g}X_2\text{/L/gTKN/L})$$

$$\alpha = \frac{\Delta NOx}{\Delta TKN} \ (\text{gNO}_x\text{/L/gTKN/L})$$

where, for a given cycle, DX_1 is the variation of carbon oxidizers, ΔX_2 is the variation of nitrogen oxidizers, ΔCOD and are the quantities of degraded COD and TKN, respectively, during this cycle and ΔNO_x is the quantity of nitrogen oxides produced during the cycle.

Finally, one measure of k_La was realized for each set and the value for S_O^{SA} is directly obtained form the dissolved oxygen curve. The identified parameters for the identification data sets are reported in table 2.

Table 2 : Specific characteristics of the data sets used for model identification

File name (date)	k_La (min^{-1})	S_O^{SA} (g/L)	Y_1 (gX_1/gDCO)	Y_2 (gX_2/gNTK)	α (g NO/gTKN)
12112003	0.16	0.0058	1.21	0.787	0.33
08072003	0.24	0.007	0.968	0.6	0.53
06112003	0.39	0.0088	1.912	0.771	0.51
04112003	0.31	0.0068	1.306	0.885	0.487
29102003	0.31	0.0087	2.105	0.919	0.3
26062003	0.24	0.00787	1.015	0.557	0.57
15042004	0.24	0.0061	2.246	0.657	0.64
10072003	0.24	0.0072	0.856	1.236	0.73
06082003	0.24	0.0062	1.778	0.828	0.43
			Mean : 1.489 STD[1] : 0.53	Mean : 0.804 STD : 0.20	Mean : 0.50 STD : 0.14

[1] Standard Deviation

It should be noticed that the parameters related to the O_2 (k_La and O_2^{SA}) are specific to each data sets while the mean values for Y_1, Y_2 and a will be used in the models developed hereafter (for each model, we will precise which values are used for the identification step).

3.1.4 Experimental data sets used for model validation

Six additional data sets were used for model validation. The individual characteristics of these data are reported in the table 3.

Table 3 : Characteristics of the data sets used for model validation

File name (date)	k_La (min-1)	O_2^{SA} (mg/L)	Total COD input (mg/L)	TKN input (mg/L)	SVM (g/L)
05082003	0.24	7	2,403	173	13.5
06042004	0.24	6.1	6,504	231	12.3
21042004	0.24	5.8	5,312	154	14.4
25032004	0.24	7.5	5,259	212	11.3
27102003	0.31	9.4	5,090	168	15.8
31102003	0.31	7.2	5,298	204	13.5

3.1.5 Identification methods and pre-treatment of data

An example of the raw experimental data set used for model identification is plotted in the figure 3.

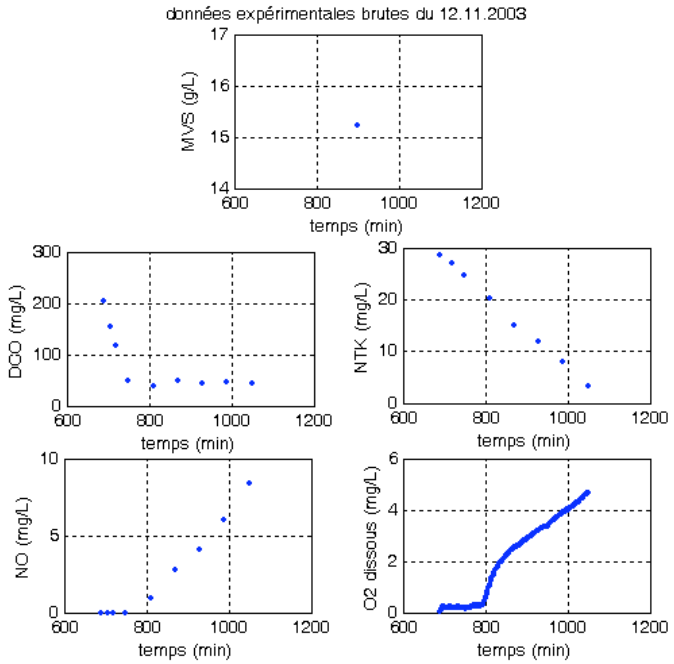

Figure 3 : Raw experimental data of 12.11.2003 (file 12112003)

As can be seen, about ten points are available relatively to the COD, TKN and NO_x. The sample time for oxygen is 2 minutes. One additional measurement is taken : it is the total biomass concentration at the end of the cycle. However, since this measurement is quite uncertain and because only one point per cycle is available, it is only used to compute the "most probable" concentration of the initial total biomass and it is not used within the optimization criterion which is expressed as :

$$J = \sum_{i=1}^{9} J_i$$

with

$$J_i = \sum_{j=1}^{n_{COD}(i)} p_{COD}(i,j)\left(S_1(t_j) - \hat{S}_1(t_j)\right) + \sum_{j=1}^{n_{TKN}(i)} p_{TKN}(i,j)\left(S_2(t_j) - \hat{S}_2(t_j)\right) + \sum_{k=1}^{n_{O_2}(i)} p_{O_2}(i,k)\left(S_O(t_k) - \hat{S}_O(t_k)\right)$$

where J is the sum of the criteria obtained for each of the nine data files available for the parameter identification, $p_{COD}(i,j)$, $p_{TKN}(i,j)$ and $p_{O2}(i,k)$ are the weights associated with the j^{th} measurements of COD, TKN and with the k^{th} measurement of O_2 that are taken at instants t_j (for COD and TKN) and at t_k for O_2 while $n_{COD}(i)$, $n_{TKN}(i)$ and $n_{O2}(i)$ are the number of experimental data available in the i^{th} data set.

The algorithm used for identification is a simplex method available in standard numerical softwares (MATLAB was used here).

In order to avoid any problem with steady state non zero values of the variables in the models, it should be noticed here that the non biodegradable fraction of COD and nitrogen are removed from the data. Thus, if we note S_1 the organic carbon. (mg COD /l) and S_2 the Ammonium nitrogen concentration (mg N-NH4/l), the models developed hereafter will be built with S_1=$COD_{biodegradable}$=COD-COD_{min} and S_2=$TKN_{biodegradable}$=TKN-TKN_{min} where COD_{min} and TKN_{min} are the non biodegradable COD and Total Nitrogen.

3.2 Modelling

As underlined above, a biological reactor with microorganisms able to perform carbon and nitrogen removal under adequate conditions of temperature, pH, is considered.

Recall the following notations for the concentrations :

X_1 : Carbon oxydisers microorganisms concentration (mg/l)

X_2 : Nitrogen oxydisers microorganisms concentration (mg/l)

S_1 : Organic carbon concentration (mg COD /l)

S_2 : Total Kejdhal Nitrogen concentration (mg N-NH4/l)

S_3 : Nitrates+Nitrites nitrogen concentration (mg N-NO3/l+ mg N-NO2/l)

S_O : Dissolved oxygen concentration (mg O_2/l)

The reaction network is given by :

$$S_1 + O_2 \xrightarrow{\varphi_1} X_1 \tag{1}$$

$$S_2 + O_2 \xrightarrow{\varphi_2} X_2 + S_3 \tag{2}$$

In the wastewater, nitrogen is essentially under organic form. It is rapidly ammonified into NH_4^+. During the biological reactions the ammonium is transformed into nitrogen gas N_2 in two steps: nitrification and denitrification (Henze and al., 1987). Nitrification is realized by Autotrophic bacteria under aerobic conditions (reaction 2). It is a two step reaction : nitritation where ammonium is converted into nitrites NO_2^- and nitratation where nitrites are converted into nitrates NO_3^-. In order to simplify the model, these two reactions are usually grouped together in one reaction where ammonium is directly converted into nitrates by Autotrophic bacteria X_2 with the growth rate $\varphi_2(.)$.

Denitrification is reducing nitrates into nitrogen gas. This reaction is done by Heterotrophic bacteria under anoxic conditions (presence of NO_3^-, absence of O_2). This bacteria uses nitrites as electron acceptor when no oxygen is available. This reaction only takes place if organic carbon is available. In anoxic condition the heterothrophic growth rate is given by $\varphi_3(.)$.

Carbon removal is realized by Heterotrophic bacteria (Henze and *al*., 1987). Carbon can be eliminated either under anoxic conditions with nitrates in denitrification phase (reaction 3) or under aerobic conditions (reaction 1). In the last case, the growth rate of Heterotrophic is $\varphi_1(.)$. In order to have the three reactions in the same tank, we should consider two sub-phases reactions : aerobic sub-phase to nitrify the nitrogen and an anoxic sub-phase to denitrify it. The carbon is eliminated in both cases.

In this section, a general reduced order state space model for the description of the SBR activated sludge process is proposed. The modelling is based on the mass balance in the reactor during the aerobic phase in neglecting the mortality terms. Thus, we consider only the apparent net growth rate of the biomass. In addition, what can happen biologically during the settling phase is neglected. Considering the reaction scheme (1 and 2), we can apply the mass balance principle to determine the state space model for both anoxic and aerobic phases.

$$\frac{dX_1}{dt} = \mu_1(S_1, S_O)X_1 \tag{3}$$

$$\frac{dX_2}{dt} = \mu_2(S_2, S_O)X_2 \tag{4}$$

$$\frac{dS_1}{dt} = -\frac{1}{Y_1}\mu_1(S_1, S_O)X_1 \tag{5}$$

$$\frac{dS_2}{dt} = -\frac{1}{Y_2}\mu_2(S_2, S_O)X_2 \tag{6}$$

$$\frac{dS_3}{dt} = \frac{\alpha}{Y_2}\mu_2(S_2, S_O)X_2 \tag{7}$$

$$\dot{S}_O = k_L a\left(S_O^{SA} - S_O\right) - \beta\mu_1\left(S_1, S_O\right)X_1 - \gamma\mu_2\left(S_2, S_O\right)X_2 \quad (8)$$

where almost all terms have already been defined: S_3 is the Nitrites+Nitrates concentration (also noted NO_x), β is the stoichiometric coefficient for the consumption of oxygen by the carbon oxidisers (g of O_2 per g of X_1) and γ is the stoichiometric coefficient for the consumption of oxygen by the nitrogen oxidisers (g of O_2 per g of X_2).

3.3 Model identification

3.3.1 Models # 1 & #2

Structure of the models #1 & #2
The structure of the first model to be first considered is given by :

$$\dot{X}_1 = \mu_{1\max}\frac{S_1}{S_1 + K_1}\frac{S_O}{S_O + K_{O1}}X_1 \quad (9)$$

$$\dot{X}_2 = \mu_{2\max}\frac{S_2}{S_2 + K_2}\frac{S_O}{S_O + K_{O2}}X_2 \quad (10)$$

$$\dot{S}_1 = -\frac{1}{Y_1}\mu_{1\max}\frac{S_1}{S_1 + K_1}\frac{S_O}{S_O + K_{O1}}X_1 \quad (11)$$

$$\dot{S}_2 = -\frac{1}{Y_2}\mu_{2\max}\frac{S_2}{S_2 + K_2}\frac{S_O}{S_O + K_{O2}}X_2 \quad (12)$$

$$\dot{S}_3 = \frac{\alpha}{Y_2}\mu_{2\max}\frac{S_2}{S_2 + K_2}\frac{S_O}{S_O + K_{O2}}X_2 \quad (13)$$

$$\dot{S}_O = k_L a\left(S_O^{SA} - S_O\right) - \beta\mu_{1\max}\frac{S_1}{S_1 + K_1}\frac{S_O}{S_O + K_{O1}}X_1 - \gamma\mu_{2\max}\frac{S_2}{S_2 + K_2}\frac{S_O}{S_O + K_{O2}}X_2 \quad (14)$$

where μ_{1max} and μ_{2max} are the maximum specific growth rates of carbon and nitrogen oxidisers respectively (in min^{-1}), K_1 and K_2 are the saturation coefficient for S_1 and S_2 of the double Monod functions (g/l), K_1 and K_2 are the saturation coefficient for the oxygen of the double Monod functions for X_1 and X_2, respectively (g/l).

As underlined above, a number of parameters were directly computed from the raw experimental data. The values for Y_1, Y_2 and α are the mean values reported in the Table 2 while the values for k_La and S_O^{SA} are specific to each data set. These parameter values are reported in the second and third columns of the Table 2 for the experimental data sets used for model parameter identification and in the second and third columns of the Table 3 for the data used for model validation. Prior to report the results of the identification, it was verified that the parameters were identifiable in running the optimization algorithm with different initial values for the parameters. Following this study, it was not possible to conclude to the global identifiability of the model. However, in a quite large range around the actual initial conditions chosen for the parameters, the algorithm converged toward identical values.

Model #1 and #2 identification

At this step, eleven models were identified : the nine first models (noted model #1.*i*, *i*=1…9) were obtained in minimizing the J_i criteria presented in the section "Identification methods and pre-treatment of data", the model #1.10 is the "mean" of these models while the eleventh model (noted #2) was obtained in minimizing the criterion J using all the available identification experimental data.

- Nine different models denoted 1.*i*, *i*=1…9, corresponding to one identified parameter set by data set. The identified parameter values are reported in the appendix. One model (noted model #1.10) simply consists in the "mean" of the first nine previously identified models. The parameters values of this model are reported in the appendix.
- Finally, an additional model (noted model #2) was identified using all the available experimental data sets. For this last models, the mean values for Y_1, Y_2 and α reported in the table 2 were used. The identification results are reported in the table 6 in the appendix and examples of results are shown in Figures 4a to 4d.

Because the first 9 models have very few practical interest, only identification results obtained with models #1.10 and 2 are given.

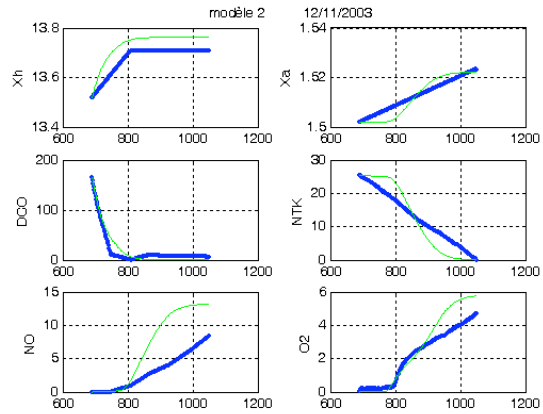

Figure 4a : Raw experimental data and simulations of 12.11.2003 (file 12112003)

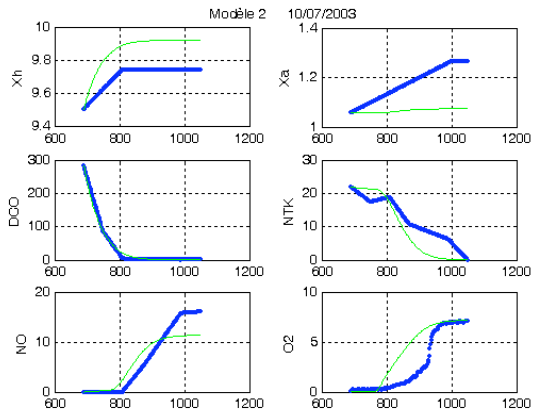

Figure 4b : Raw experimental data and simulations of10.07.2003 (file 10072003)

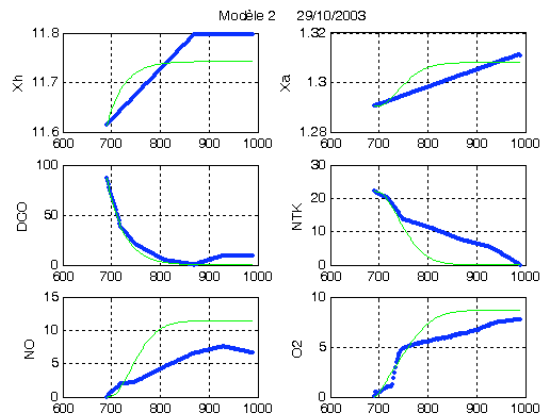

Figure 4c : Raw experimental data and simulations of 29.10.2003 (file 29102003)

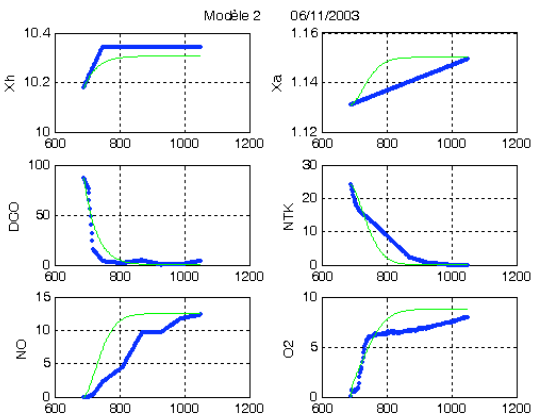

Figure 4d : Raw experimental data and simulations of 06.11.2003 (file 06112003)

3.3.2 Model #3

Structure of the model #3

Let us investigate now whether the first model structure of models #1 and #2 can be simplified and under which assumptions given that our objective is to derive the simplest possible model which captures with "sufficient accuracy" the dynamics of the system.

As shown in the figures 5, 6 and 7, the first simplifications to be realized are concerned with the expressions of the X_1 and X_2 kinetics. Concerning the growth rate of X_1, the values of K_1 and K_{O1} allows us to propose the simple expression :

$$\mu_1(S_1, S_O) = \mu_{1\max} S_1 S_O \tag{15}$$

for its kinetics while the value of K_2 allows one to replace μ_2 by :

$$\mu_2(S_2, S_O) = \mu_{2\max} S_2 \frac{S_O}{S_O + K_{O2}} \tag{16}.$$

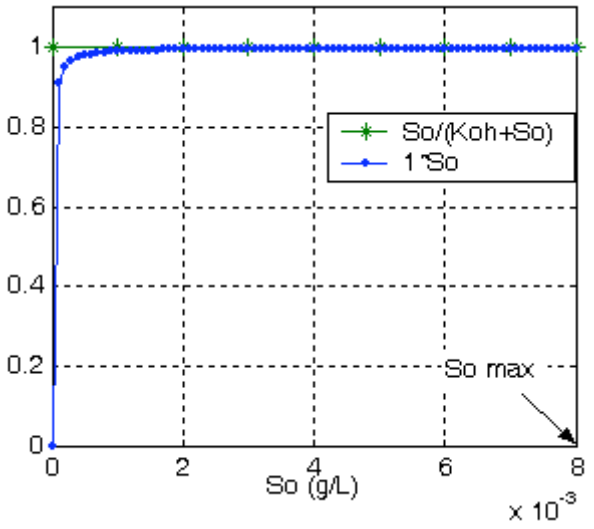

Figure 5 : Comparison between a Monod and linear kinetics for the oxygen (first biomass)

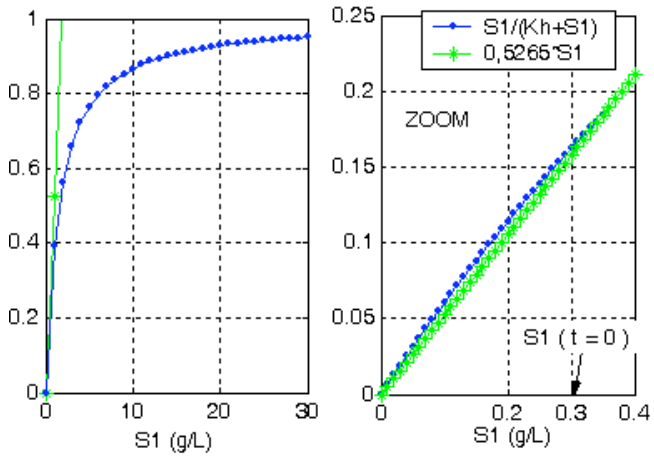

Figure 6 : Comparison between a double and a single Monod kinetics function for the first biomass

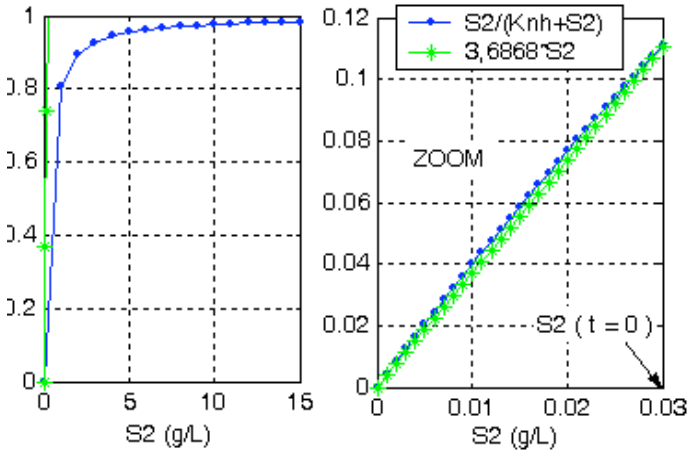

Figure 7 : Comparison between a double and a single Monod kinetics function for the second biomass

The final structure of the model #3 to be retained is thus :

$$\dot{X}_1 = \mu_{1\max} S_1 S_O X_1 \tag{17}$$

$$\dot{X}_2 = \mu_{2\max} S_2 \frac{S_O}{S_O + K_{O2}} X_2 \tag{18}$$

$$\dot{S}_1 = -\frac{1}{Y_1} \mu_{1\max} S_1 S_O X_1 \tag{19}$$

$$\dot{S}_2 = -\frac{1}{Y_2} \mu_{2\max} S_2 \frac{S_O}{S_O + K_{O2}} X_2 \tag{20}$$

$$\dot{S}_3 = \frac{\alpha}{Y_2} \mu_{2\max} S_2 \frac{S_O}{S_O + K_{O2}} X_2 \tag{21}$$

$$\dot{S}_O = k_L a \left(S_O^{SA} - S_O\right) - \beta \mu_{1\max} S_1 S_O X_1 - \gamma \mu_{2\max} S_2 \frac{S_O}{S_O + K_{O2}} X_2 \tag{22}$$

Model #3 identification

Because of the simplications, using only one data set would certainly lead to a very high uncertainty on the parameters. This is why, from now upwards, the model parameters are identified using the nine sets of available experimental data. The results of the identification with the structure of the model #3 are reported in the table 7 in the appendix while the figures 8 represent a number of comparisons between simulated data and experimental ones.

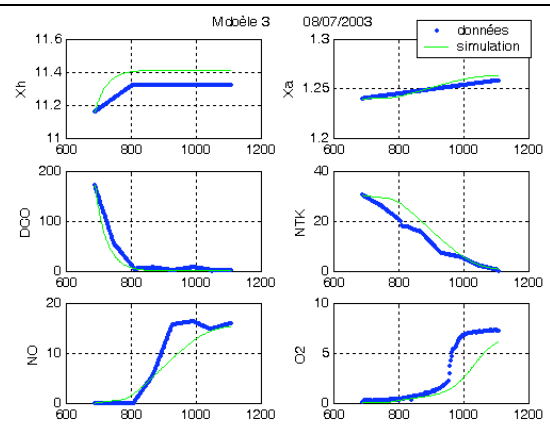

Figure 8a : Raw experimental data and simulated ones (file 08072003)

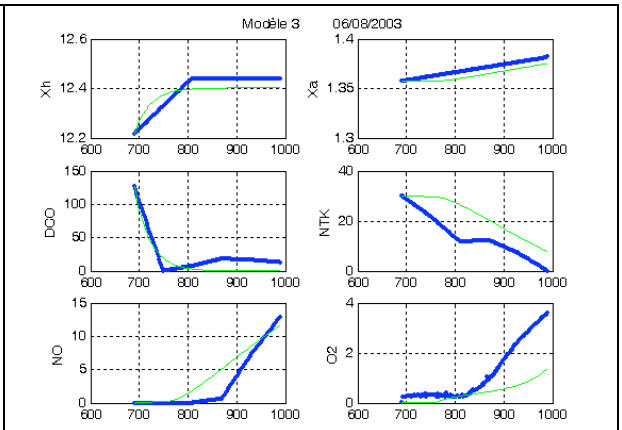

Figure 8b : Raw experimental data and simulated ones (file 06082003)

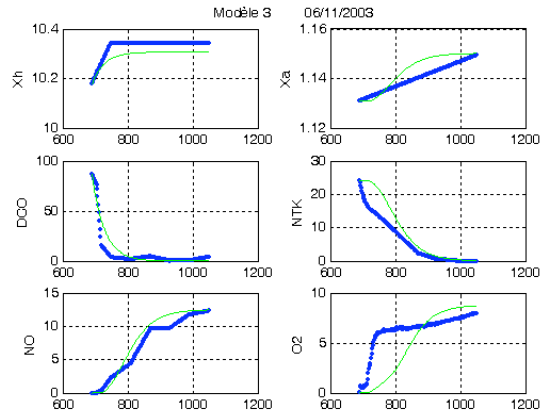

Figure 8c : Raw experimental data and simulated ones (file 06112003)

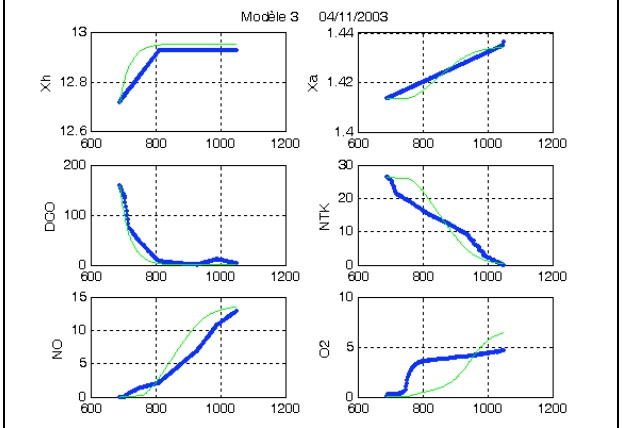

Figure 8d : Raw experimental data and simulated ones (file 04112003)

3.3.3 Model #4

Structure of the model #4

Two further simplications are now made : first, it is assumed that the oxygen concentration is never limiting. Thus, the growth rates are simply linear functions of S1 and S2 respectively. Furthermore, given the very high concentration of total biomass at which the experiments were realized, it is assumed that the quantity of biomass produced during one cycle is negligible and it is simply considered to be constant over one cycle. The structure of model #4 is then given by the following linear equations :

$$\dot{S}_1 = -\frac{1}{Y_1}\mu_{1\max}S_1 \tag{23}$$

$$\dot{S}_2 = -\frac{1}{Y_2}\mu_{2\max}S_2 \tag{24}$$

$$\dot{S}_3 = \frac{\alpha}{Y_2}\mu_{2\max}S_2 \tag{25}$$

$$\dot{S}_O = k_L a\left(S_O^{SA} - S_O\right) - \beta\mu_{1\max}S_1 - \gamma\mu_{2\max}S_2 \tag{26}$$

which can simply be rewritten in a state space form as :

$$\begin{bmatrix} \dot{S}_1 \\ \dot{S}_2 \\ \dot{S}_3 \\ \dot{S}_O \end{bmatrix} = \begin{bmatrix} -\frac{1}{Y_1}\mu_{1\max} & 0 & 0 & 0 \\ 0 & -\frac{1}{Y_2}\mu_{2\max} & 0 & 0 \\ 0 & \frac{\alpha}{Y_2}\mu_{2\max} & 0 & 0 \\ -\beta\mu_{1\max} & -\gamma\mu_{2\max} & 0 & -k_L a \end{bmatrix} \begin{bmatrix} S_1 \\ S_2 \\ S_3 \\ S_O \end{bmatrix} + \begin{bmatrix} 0 \\ 0 \\ 0 \\ k_L a S_O^{SA} \end{bmatrix} \quad (27)$$

Model #4 identification

Although there exists plenty of numerical methods to identify linear models, the same algorithms than before are used to identify the model #4. The results are presented in the table 8 in the appendix while different corresponding figures are represented in the figures 9.

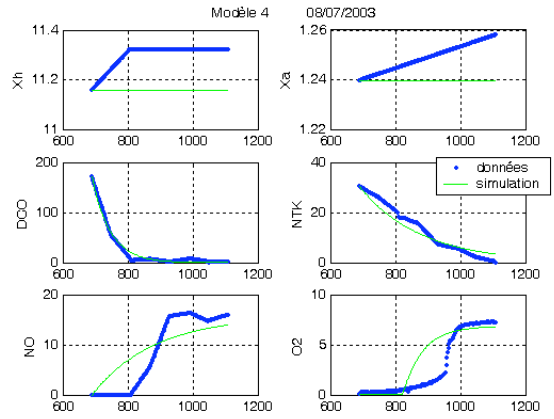

Figure 9a : Raw experimental data and simulated ones (file 08072003)

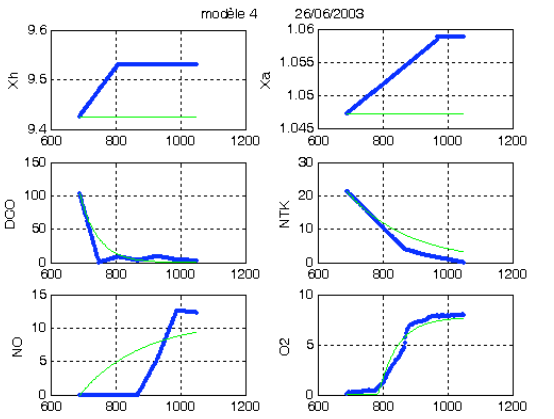

Figure 9b : Raw experimental data and simulated ones (file 26062003)

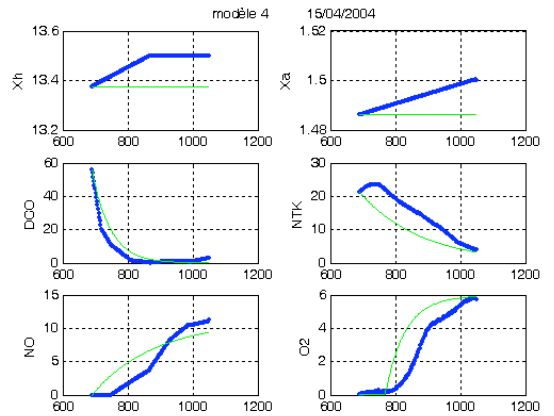

Figure 9c : Raw experimental data and simulated ones (file 15042004)

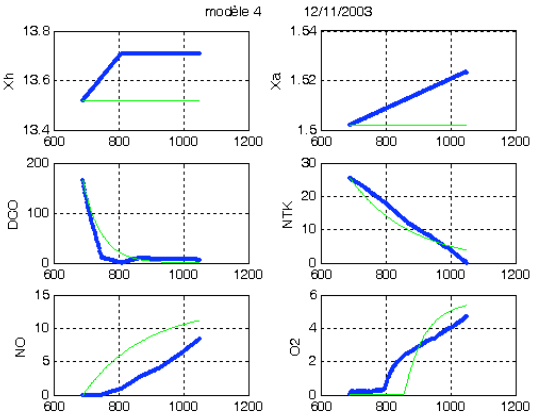

Figure 9d : Raw experimental data and simulated ones (file 12112003)

Remarks : the accuracy in the identification of the parameters should be discussed. It should be noticed that the small number of available data (only one experimental data set, that is about 20 data for the COD and the TKN and the dissolved oxygen) make the uncertainty on the identified value to be very high. Thus, a number of values have simply nonsense : it is the case, for instance, for the parameter K_{O1} of the data set 29.10.2003 which is found to be equal to $0 \pm 2.2 \times 10^{-3}$, and as such, includes possible negative values. For other parameters and data sets, the uncertainty is higher, in magnitude, than the value itself : it is the case for example for the parameter K_1 of the model #1.5 which is equal to $9.08 \times 10^{-1} \pm 3.77$.

3.4. Validation

Once established, the models were validated with the validation data sets. The results are presented in the following figures.

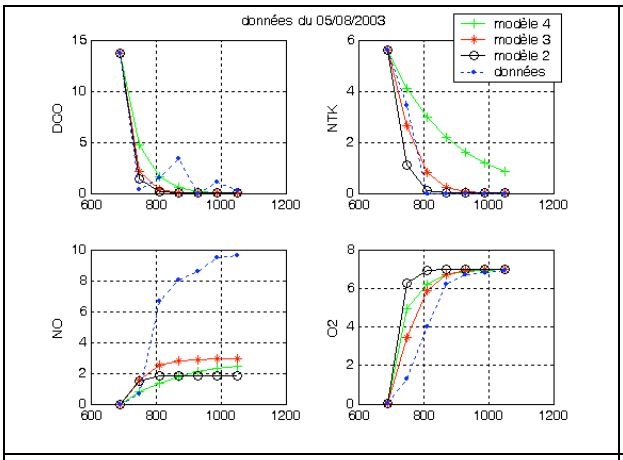

Figure 10a : Raw validation experimental data and simulations for models #1 to #4 (file 12112003)

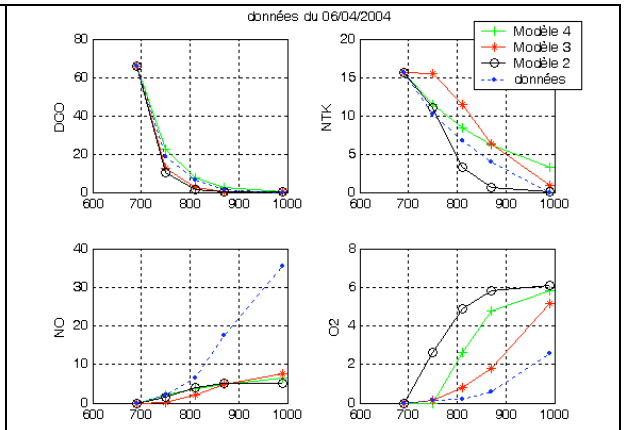

Figure 10b : Raw validation experimental data and simulations for models #1 to #4 (file 12112003)

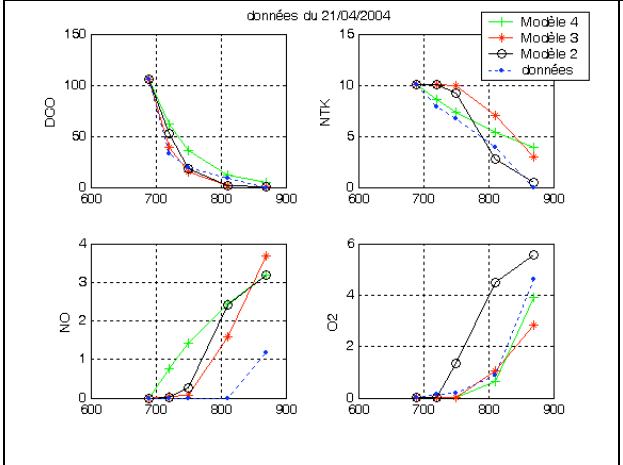

Figure 10c : Raw validation experimental data and simulations for models #1 to #4 (file 12112003)

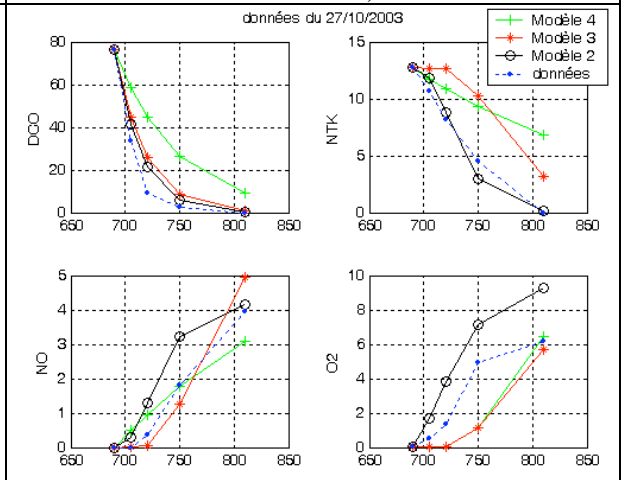

Figure 10d : Raw validation experimental data and simulations for models #1 to #4 (file 12112003)

4. Conclusions

For the EM1 model it was possible to estimate a set of parameters for a mass-balance based model that reflects the most important behavior of the process with the minimum of complexity. The confidence intervals for the calibration of the parameters lie within 7% of their respective mean value.

A very simple mass balance model for Sequencing Batch Reactors used for the biological treatment of organic carbon and nitrogen is given for EM2. This model is intended to be used for control purposes. As such, the degree of details required is not too high and only major biological processes are taken into account. This model is identified and validated with real data acquired on a SBR pilot plant operating in the LBE, Narbonne, France. The experiments were performed in three periods of the year: Jun-July 2003, November-October 2003 and Mars-April 2004. Eight experiments are used for model parameter identification. Data of 7 other experiments are used for model validation. A modified growth function is proposed to be investigated as perspectives to adapt the model and to avoid the static error between the model and the COD measurements at the end of the aerobic phase.

REFERENCES

AFNOR, Évaluation en milieu aqueux de la biodégradabilité aérobie «ultime» des produits organiques solubles. *Normalisation Française*, NFT. 90-312 (1985)

Bastin, G. and D. Dochain (1990). *On-line estimation and adaptive control of bioreactors*, Amsterdam, Oxford, New York, Tokyo: Elsevier.

Dochain, D. and P. A. Vanrolleghem (2001). *Dynamical Modelling and Estimation in Wastewater Treatment Processes*, IWA Publishing.

Henze, M., W.Gujer, T.Mino and M. Von Loosdrecht (1987). *Activated Sludge Model N° 1*, International Association on Water Pollution Resarch and Control (IAWPRC) Scientific and Technical Report 1.

Jeppsson, U. (1996) *Modeling Aspects of Wastewater Treatment processes,* Lund, Sweden 1996.

Kargi, F. and A. Uygur (2003). Effect of carbon source on biological nutrient removal in a sequencing batch reactor, *Bioressource Technologiy* **89(1)**, pp.89-93.

Krishna, C. and C.M Van Loosdrecht (1999). Substrate Flux Storage and Growth in relation to activated sludge modeling. *Water Research* **33**, 3149 – 3161.

Orhon, D. and D. Okutman (2003). Respirometric assessment of residual organic matter for domestic sewag*. Enzyme and microbial technology* **32**, 550-566.

Sozen, S., E. Cokgor, D. Orhon and M. Henze (1998). Respirometric analysis of Activated sludge Behaviour-II Heterotrophic Growth under aerobic and anoxic condition*. Water research* 32, 476-488.

Wilderer, P.A., R.L Irvine and M.C. Goronszy (2001). *Sequencing Batch Reactor technology*, IAWPRC scientific and Technical Report 10.

APPENDIX

Table 4 : Parameter values for each file for model #1

Model #1.i, i=1…9	Model 1.1	Model 1.2	Model 1.3
Data file	12.11.2003	08.07.2003	06.11.2003
μ_{1max}	$6.5\times10^{-3}\pm1.23\times10^{-2}$	$7.1\times10^{-3}\pm1.00\times10^{-2}$	$1.94\times10^{-2}\pm8.6\times10^{-3}$
K_1	$9.04\times10^{-1}\pm1.66$	1.41 ± 1.98	$9.02\times10^{-1}\pm4.9\times10^{-1}$
K_{O1}	$8\times10^{-4}\pm5\times10^{-4}$	$3.3\times10^{-3}\pm2.1\times10^{-3}$	$1.0\times10^{-2}\pm4.5\times10^{-3}$
μ_{2max}	$4.3\times10^{-1}\pm7.8\times10^{-3}$	$6.8\times10^{-3}\pm6.8\times10^{-3}$	$4.7\times10^{-3}\pm2.2\times10^{-3}$
K_2	$1.43\times10^{-1}\pm1.69\times10^{-1}$	$3.0\times10^{-1}\pm4.0\times10^{-1}$	$1.47\times10^{-1}\pm7.28\times10^{-2}$
K_{O2}	$2.92\times10^{-2}\pm5.21\times10^{-2}$	$3.0\times10^{-2}\pm5.17\times10^{-2}$	$1.96\times10^{-2}\pm1.18\times10^{-2}$
β	$2.19\times10^{-1}\pm1.58\times10^{-2}$	$6.34\times10^{-1}\pm6.67\times10^{-2}$	$2.32\times10^{-1}\pm9.22\times10^{-2}$
γ	$3.40\pm8.1210\times10^{-1}$	3.41 ± 2.30	3.40 ± 1.75

Model #1.i, i=1…9	Model 1.4	Model 1.5
Data file	04.11.2003	29.10.2003
μ_{1max}	$2.9\times10^{-2}\pm3.03\times10^{-2}$	$4.1\times10^{-3}\pm1.52\times10^{-2}$
K_1	$1.48\pm9.59\times10^{-1}$	$9.08\times10^{-1}\pm3.77$
K_{O1}	$9.3\times10^{-3}\pm1.01\times10^{-2}$	$0\pm2.2\times10^{-3}$
μ_{2max}	$4.29\times10^{-2}\pm3.59\times10^{-2}$	$4.2\times10^{-3}\pm3.26\times10^{-2}$
K_2	$3.0\times10^{-1}\pm3.08\times10^{-1}$	$1.62\times10^{-1}\pm4.2\times10^{-1}$
K_{O2}	$3.0\times10^{-2}\pm1.98\times10^{-2}$	$2.93\times10^{-2}\pm2.08\times10^{-1}$
β	$4.45\times10^{-1}\pm1.17\times10^{-1}$	$1.97\times10^{-1}\pm1.60\times10^{-1}$
γ	3.51 ± 1.56	3.40 ± 2.69

Model #1.i, i=1…9	Model 1.6	Model 1.7	Model 1.8	Model 1.9
Data file	26.06.2003	15.04.2004	10.07.2003	06.08.2003
μ_{1max}	$8.1\times10^{-3}\pm4.5\times10^{-3}$	$4.6\times10^{-3}\pm3.0\times10^{-3}$	$6.3\times10^{-3}\pm5.2\times10^{-3}$	$9.9\times10^{-3}\pm2.34\times10^{-2}$
K_1	$8.35\times10^{-1}\pm5.54\times10^{-1}$	$9.02\times10^{-1}\pm6.15\times10^{-1}$	$1.01\pm7.37\times10^{-1}$	$9.1\times10^{-1}\pm2.05$
K_{O1}	$5\times10^{-4}\pm2\times10^{-4}$	$4\times10^{-5}\pm8\times10^{-5}$	$3.2\times10^{-3}\pm2.9\times10^{-3}$	$1.7\times10^{-3}\pm3.6\times10^{-3}$
μ_{2max}	$1\times10^{-4}\pm1\times10^{-5}$	$2.6\times10^{-3}\pm3.3\times10^{-3}$	$4.7\times10^{-3}\pm1.04\times10^{-2}$	$6.0\times10^{-3}\pm1.96\times10^{-2}$
K_2	$1.20\times10^{-2}\pm2.1\times10^{-3}$	$3.0\times10^{-1}\pm1.16$	$1.56\times10^{-1}\pm2.98\times10^{-1}$	$1.43\times10^{-1}\pm3.07\times10^{-1}$
K_{O2}	$3\times10^{-5}\pm2\times10^{-5}$	$2.70\times10^{-2}\pm1.11\times10^{-1}$	$1.78\times10^{-2}\pm2.74\times10^{-2}$	$2.81\times10^{-2}\pm9.12\times10^{-2}$
β	$8.93\times10^{-1}\pm1.50\times10^{-1}$	$2.63\times10^{-1}\pm1.34\times10^{-1}$	$4.49\times10^{-1}\pm5.58\times10^{-2}$	$2.36\times10^{-1}\pm5.53\times10^{-2}$
γ	3.45 ± 2.85	3.41 ± 4.54	3.40 ± 1.62	3.40 ± 1.58

Table 5: Mean value of the parameter identified by using each data file independently

	Model 1.10
μ_{1max}	$10.6\times10^{-3}\pm5.13\times10^{-3}$
K_1	$1.03\pm1.48\times10^{-1}$
K_{O1}	$3.2\times10^{-3}\pm2.39\times10^{-3}$
μ_{2max}	$8.5\times10^{-3}\pm1.20\times10^{-3}$
K_2	$1.85\times10^{-1}\pm6.04\times10^{-2}$
K_{O2}	$2.34\times10^{-2}\pm6.13\times10^{-3}$
β	$3.96\times10^{-1}\pm1.47\times10^{-1}$
γ	$3.42\pm2.32\times10^{-2}$

Table 6: Parameter values obtained by using the nine data files simultaneously

	Model 2
μ_{1max}	$5.9\times10^{-3}\pm7\times10^{-4}$
K_1	$1.55\pm2.08\times10^{-1}$
K_{O1}	$1\times10^{-5}\pm1\times10^{-6}$
μ_{2max}	$2.16\times10^{-2}\pm4.24\times10^{-3}$
K_2	$2.40\times10^{-1}\pm5.31\times10^{-2}$
K_{O2}	$2.16\times10^{-2}\pm4.4\times10^{-3}$
β	$8.57\times10^{-1}\pm5.01\times10^{-2}$
γ	$3.42\pm3.07\times10^{-1}$

Table 7: Parameter values obtained for model #3

	Model 3
μ_{1max}	$3.8\times10^{-3}\pm0.8\times10^{-4}$
μ_{2max}	$1.71\times10^{-2}\pm1.2\times10^{-3}$
β	$2.05\pm2.14\times10^{-1}$
γ	$15.28\pm5.1\times10^{-1}$

Tableau 8 : Parameter values obtained for model #4

	Model 4
μ_{1max}	$3.8\times10^{-3}\pm0.8\times10^{-4}$
μ_{2max}	$1.71\times10^{-2}\pm1.2\times10^{-3}$
β	$2.05\pm2.14\times10^{-1}$
γ	$15.28\pm5.1\times10^{-1}$